SAE INTERNATIONAL

ARTICLE INFO
Article ID: 03-18-08-0046

doi:10.4271/03-18-08-0046

The Technological Concept of a Self-Adjusting Segmented Ceramic Sealing System for a Turboshaft Engine with Isochoric Combustion

Piotr Tarnawski[1]

[1]*Warsaw University of Technology: Politechnika Warszawska, Poland*

Abstract

The article presents self-adjusting segmented ceramic seals designed for a novel turboshaft engine operating according to the Humphrey thermodynamic cycle. The sealing system is an integral part of the developed engine concept, which features rotating isochoric combustion chambers. The seals utilize centrifugal force as the sealing force, enabling uniform sealing regardless of thermal conditions and associated deformations. The sealing consists of segments with adjustable dimensions in both circumferential and transverse directions. The sealing elements should be made of Si_3N_4 ceramic, characterized by high thermal resistance (1300°C) and low thermal expansion ($3.2 \cdot 10^{-6}$/°C). The article presents three different variants of sealing systems, differing in terms of the technological possibilities of their manufacturing. Special treatments must be applied to ensure high machining accuracy of the sealing elements. The proposed sealing system is a critical point in the design of an engine with isochoric combustion chambers. Successful sealing is key to the implementation of the Humphreys thermodynamic cycle, which offers higher engine efficiency compared to classical turboshaft engines available on the market. The article concludes with the presentation of a model for experimental investigations, along with its thermal analysis.

History

Received: 17 Apr 2025
Revised: 27 Aug 2025
Accepted: 14 Nov 2025
e-Available: 08 Dec 2025

Keywords

Pressure gained combustion, Humphrey cycle, turboshaft engine, CFD analysis, valve timing system, sealing system

Citation

Tarnawski, P., "The Technological Concept of a Self-Adjusting Segmented Ceramic Sealing System for a Turboshaft Engine with Isochoric Combustion," *SAE Int. J. Engines* 18(8):875-887, 2025, doi:10.4271/03-18-08-0046.

ISSN: 1946-3936
e-ISSN: 1946-3944

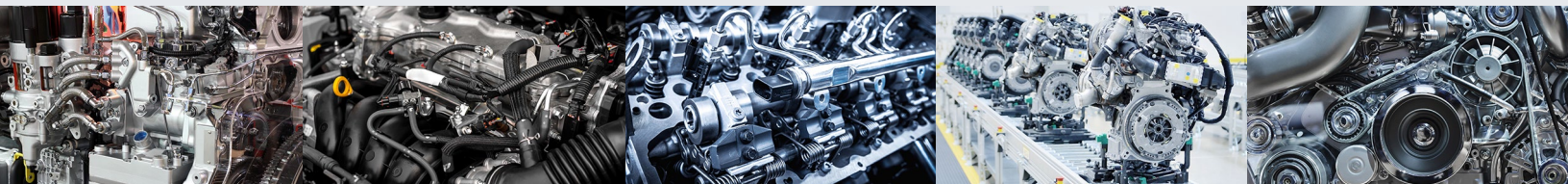

1. Introduction

1.1. Principle of Operation and Performance Parameters of the Presented Turboshaft Engine Concept

The implementation of the isochoric combustion and realization of the Humphreys cycle requires the temporary opening and closing of combustion chambers. The engine must sequentially execute the filling stage, isochoric combustion stage, and exhaust stage. The systematically developed engine concept presented in this article incorporates a timing system based on mutually rotating elements [1–3] (see Figure 1). The engine cycle is achieved using rotating combustion chambers that operate in conjunction with stationary inlet and outlet nozzles. Two stationary direct injectors are sufficient to serve six combustion chambers. The air is externally compressed—first in the turbocharger and then in the single-stage centrifugal compressor. The mechanical compressor shares a common shaft with the turbine, which operates at 35 krpm (Figure 2). Key advantages of the presented engine concept include:

- Increase of pressure in chamber during combustion stage, from 2.0 MPa to 5.2 MPa (Figure 4).
- Effective chamber filling with nearly constant pressure (as illustrated in Figures 3 and 4).
- Continuous gas flow through the nozzles and turbine, despite the engine's pulsating operation.
- Gas expansion through nozzles of varying pressure.
- Nozzles oriented at different angles to the turbine correspond to differences in gas velocity.
- Integration of a turbocharger that recovers residual kinetic energy downstream of the main turbine.

It is also worth highlighting the engine's simplicity. It features a single-stage turbine, and the injection system and turbocharger components—readily available on the automotive market—can be utilized [4–6].

The effective efficiency of the engine, as evaluated by CFD simulation, reached 32.2% for 500 kW (Table 1) and 35.0% for 1000 kW [3]. These results are highly promising, as the engine's efficiency exceeds that of conventional turboshaft engines currently available on the market. For comparison, the PWD207D—427 kW—has an efficiency equal to 25.1%, while MTR390—958 kW—reaches 29.3% [7].

FIGURE 1 CFD simulation model of turboshaft engine concept—500 kW (general and top view).

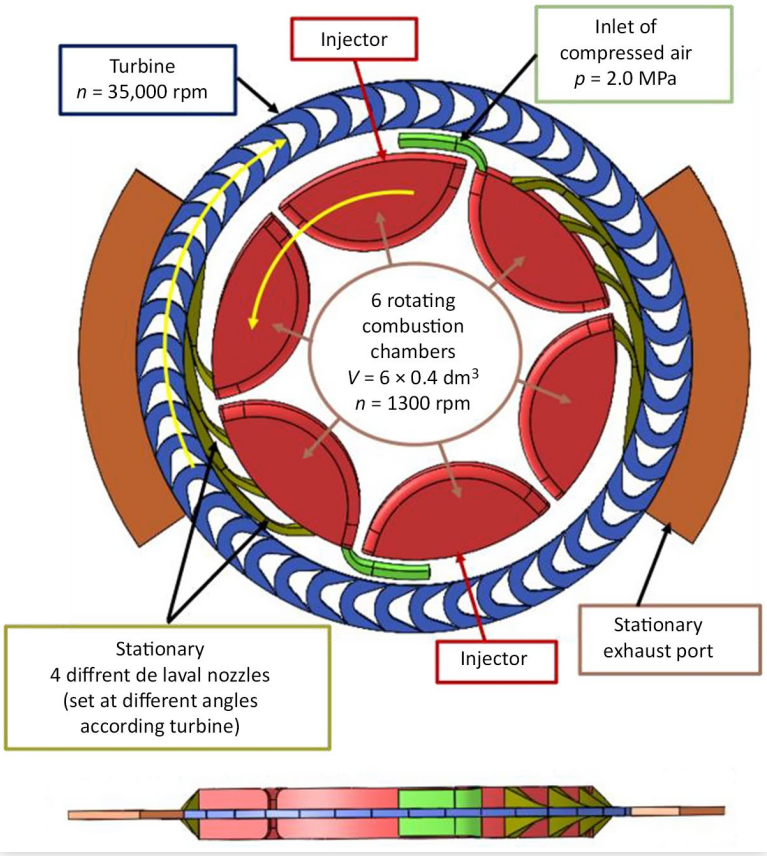

FIGURE 2 Diagram of engine concept with gas flow patch.

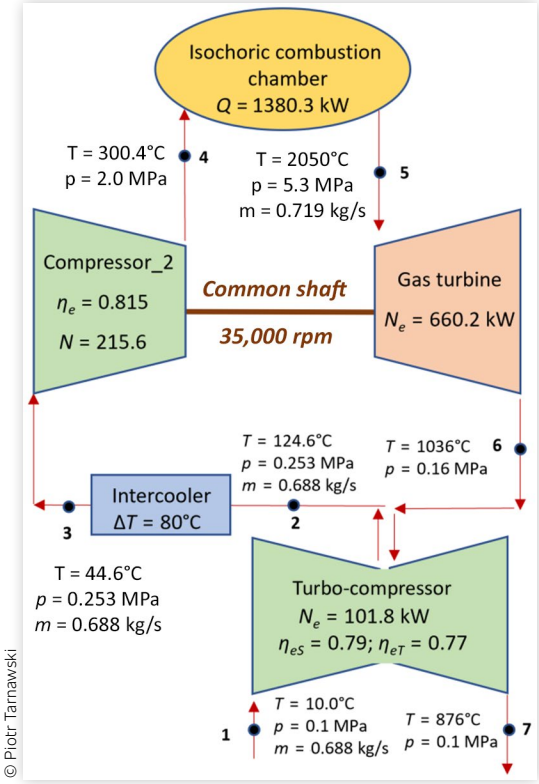

FIGURE 3 Change in oxygen content of the gas for 60 degrees of rotation of chambers (1 engine cycle).

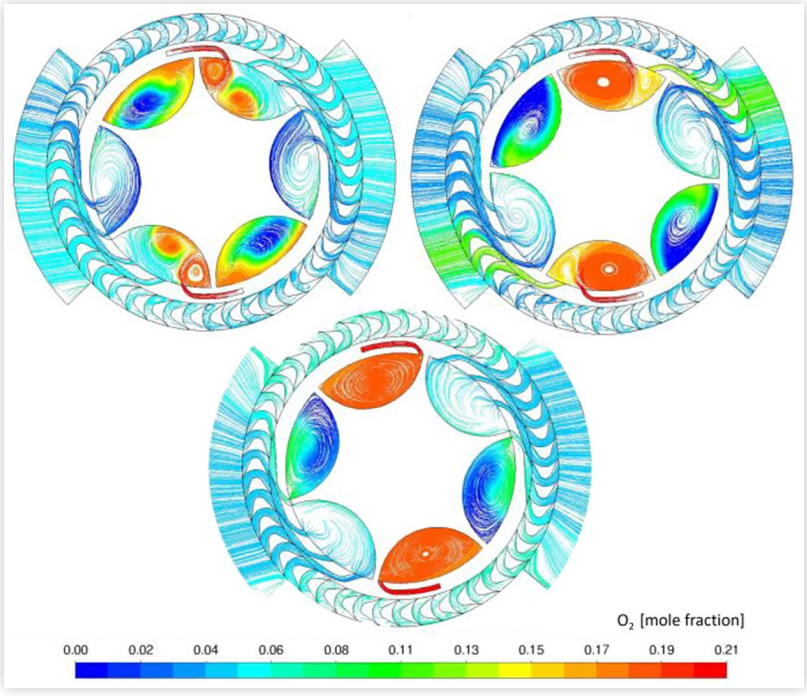

FIGURE 4 Pressure changes in combustion chambers and nozzles for two engine cycles (C1, C2, C3—three chambers, N1, N2, N3, N4—four nozzles).

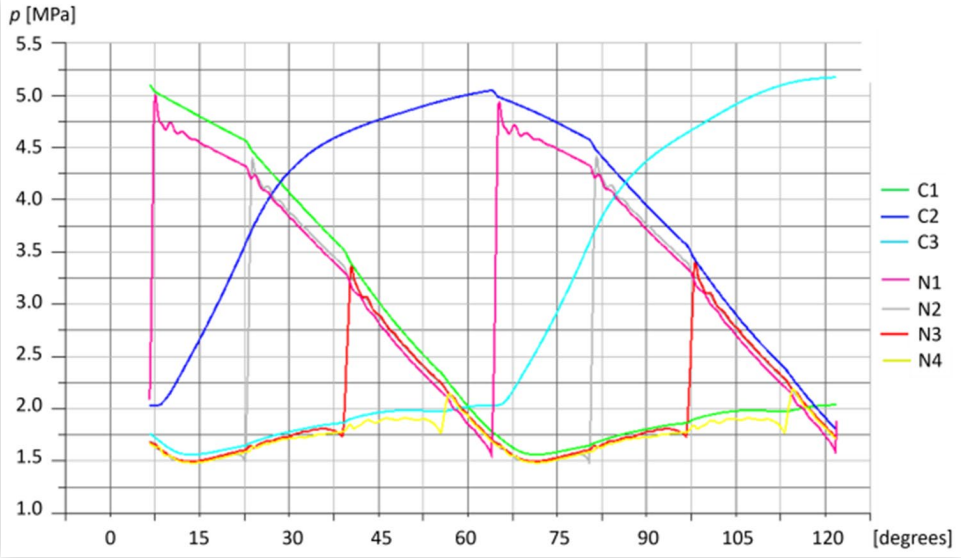

1.2. Advantages of the Presented Engine Concept over the Radial Wave Engine

The presented concept of turboshaft engine aligns with the widely researched pressure gained combustion (PGE) area, as explored by numerous authors [8–16]. Significant research efforts have been directed toward the development of the radial wave engine (RWE), illustrated in Figure 6. However, the proposed engine offers several advantages over RWE.

Notably, it requires significantly fewer combustion chambers, each with a larger volume. This design allows for an extended fresh air filling process and reduces the need for precise timing of the chamber opening and closing phases within the engine cycle. The realization of the Humphrey cycle is generally more straightforward and can be effectively achieved across a wider range of rotational speeds. This flexibility results from the elimination of additional compression via compression waves, which typically provide only marginal benefits. Additionally, the larger combustion chambers accommodate a more robust sealing system—an essential factor for the engine's overall viability. Since the intake and exhaust gases pass through the upper cylindrical surface, sealing is required on only one side of each chamber, further simplifying the design. Furthermore, the proposed engine concept allows for more effective cooling of the combustion chambers compared to the RWE.

TABLE 1 Calculated parameters of engine performance.

Parameter description	Value
The chemical energy of fuel	E_{chem} = 0.00012 kg * 2 * 44,240 kJ/kg/0.00769 s = 1380.3 kW
Effective demand for kinetic energy in turbocompressor	N_{eC_turbo} = 101.8 kW
Effective demand for work in centrifugal compressor	N_{eC_mech} = 215.6 kW
Effective work generated by gas turbine	N_{eGT} = [(189.6 Nm * 35,000 rpm)/9549] * 0.95 = 660.2 kW
Effective engine power	N_e = 660.2 – 215.6 = 444.6 kW
The effective efficiency of the engine	η_E = 444.6/1380.3 = 0.322
Specific fuel consumption	g = 2 * 0.00012 * 1000 * 3600/(0.00769 * 444.6) = 252.7 g/kWh

1.3. Sealing Challenges in Isochoric Combustion Chambers

It is worth noting that the concept of engines utilizing isochoric combustion has already been subject to experimental investigation. Two notable attempts include the prototypes developed by ABB [12] and California State Polytechnic University [13]. These projects serve as valuable case studies, highlighting both the potential and the technical challenges of this combustion strategy. Despite innovative designs, both experiments ultimately failed to achieve operational success due to unresolved sealing issues.

In particular, [12] reported several challenges: an inhomogeneous air–fuel mixture that slowed flame propagation, a peak pressure of only 0.9 MPa (compared to the expected 1.0–1.5 MPa) due to leakage, excessive thermal stress on the ignition ring, and a complex, sensitive electromechanical mechanism for managing the leakage gap. The study recommended several improvements, including

the installation of a discharge pipe to remove leaked gases, the use of an air-cooled rotor, dual-sided rotor support, and mechanical control of thermal expansion.

In the work presented in [13] a spring-loaded seal was implemented between the outer rotor casing and the rotor. This sealing system involved machining a pocket into the outer end wall of the casing, into which a thin annular insert was placed, positioned between the rotor tip and the casing. To secure the insert in place relative to the casing, multiple screws were used, each paired with a spring to apply consistent pressure. In practice, the insert material could be selected from a range of options, including metals, metal alloys, composites, or ceramics. For experimental purposes, Teflon was used due to its non-abrasive properties, offering protection against potential damage to the rotor blade tips. However, Teflon exhibited satisfactory performance only during short-term combustion tests, indicating limited thermal and mechanical durability under prolonged operation.

2. Materials and Methods

2.1. Concept of Construction of Turboshaft Engine

The engine concept presented in this article demonstrates strong potential for practical implementation, particularly due to its innovative sealing system. It relies on the centrifugal force, not on the elastic properties of the materials.

In conjunction with the CFD model, a detailed engine construction concept was developed (Figure 5). The design features two independent shafts operating at different rotational speeds. The first shaft, rotating at 1.3 krpm, is responsible for driving the combustion chambers and is intended to be powered by an electric motor. The second shaft, rotating at 35 krpm, is connected to the turbine and is tasked with delivering mechanical power output. The primary structural components of the engine are illustrated in Figure 5, however, the turbocharger and centrifugal compressor are not shown.

The engine requires sealing in two critical locations. The self-adjusting segmented ceramic seal is employed for sealing the combustion chambers, while a labyrinth seal is used for the turbine. The peripheral labyrinth seal is particularly suitable for high-speed turbines, where the operating pressure is considerably lower than in the combustion chambers [17, 18]. Given the high pressure within the combustion chambers (exceeding 5 MPa) and the unique structural layout of the engine, a novel sealing solution was necessary (Figure 6). This original system is designed to ensure tight sealing both along the circumference of each chamber and between adjacent chambers, where significant pressure differentials exist.

2.2. Principle of Operation of Self-Adjusting Seals

The self-adjusting segmented ceramic sealing system is an indispensable element of the presented engine

FIGURE 5 Concept of construction of engine (500 kW—specification of elements).

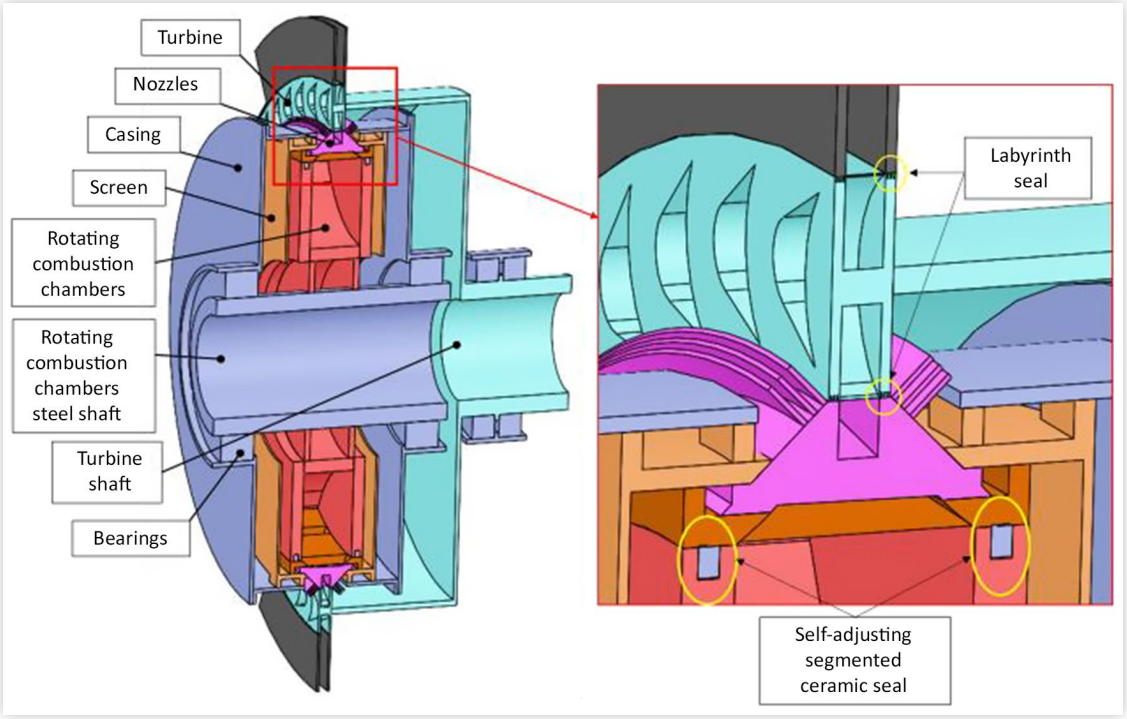

FIGURE 6 Isochoric combustion chambers with self-adjusting segmented ceramic sealing system—engine 500 kW.

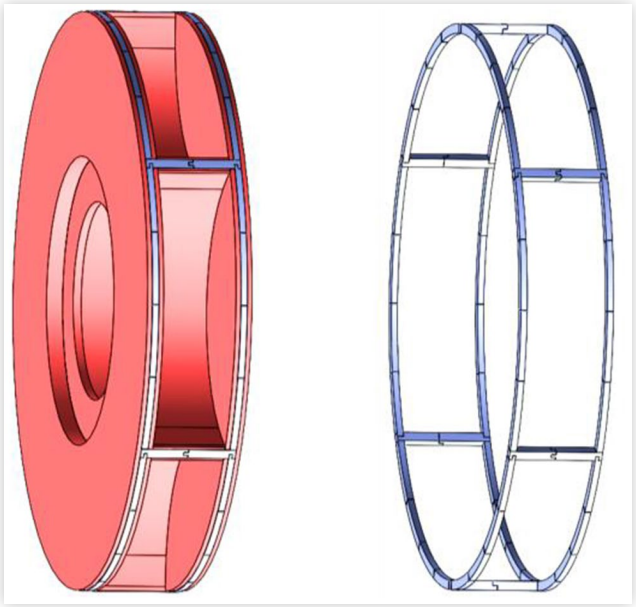

concept. It consists of combustion chambers, segment-sealing elements, and casing (see Figure 7). All components should be made from the same Si_3N_4 ceramic material, which can withstand high temperatures (1300°C), has a low thermal expansion ($3.2 \cdot 10^{-6}$/°C), and high hardness (18 GPa) [19–21]. The segment-sealing elements are placed in grooves formed within the combustion chambers. The circumferential seals prevent the leakage of high-pressure gases to the outside, while the transverse seals prevent leakage between chambers (see Figure 8). Due to the centrifugal force generated by the rotational motion of the chambers, the seals are pushed out of the grooves and pressed against the stationary counter-surface of the casing. The seals can adapt to potential variations in the gap between the chambers and the counter-surface. Since the sealing system is equipped with adjustment locks (see Figures 8 and 9), it can compensate for dimensional changes in both the circumferential and transverse directions. This ensures consistent seal thickness regardless of thermal conditions and the resulting deformations. Additionally, due to friction, the segment seals press against each other along the circumference, further maintaining the seal thickness.

2.3. Friction Work of Seals

The centrifugal force generates a constant pressure that pushes the seals against the counter-surface of the casing. The total pressing force exerted by all segments was 647.7 N, as calculated using Equation 1. With 60 segments in the sealing system, the force acting on a single segment was equal to 10.7 N.

$$F_c = m \cdot \omega^2 \cdot R \tag{1}$$

where F_c [N]—centrifugal force, m = 0.2 kg—sum mass of all segment seals, ω = 136.14 rad/s—angular velocity, R = 0.175 m—radius.

The sealing system can operate either dry or with lubrication using high-temperature copper grease. The grease should be applied in small quantities and at low pressure through two or three circumferential holes in the casing. The friction force during dry operation was 129.5 N, while during lubricated operation it was 32.4 N. These values were calculated using Equation 2.

$$F_f = \mu \cdot F_c \tag{2}$$

FIGURE 7 Elements of sealing system.

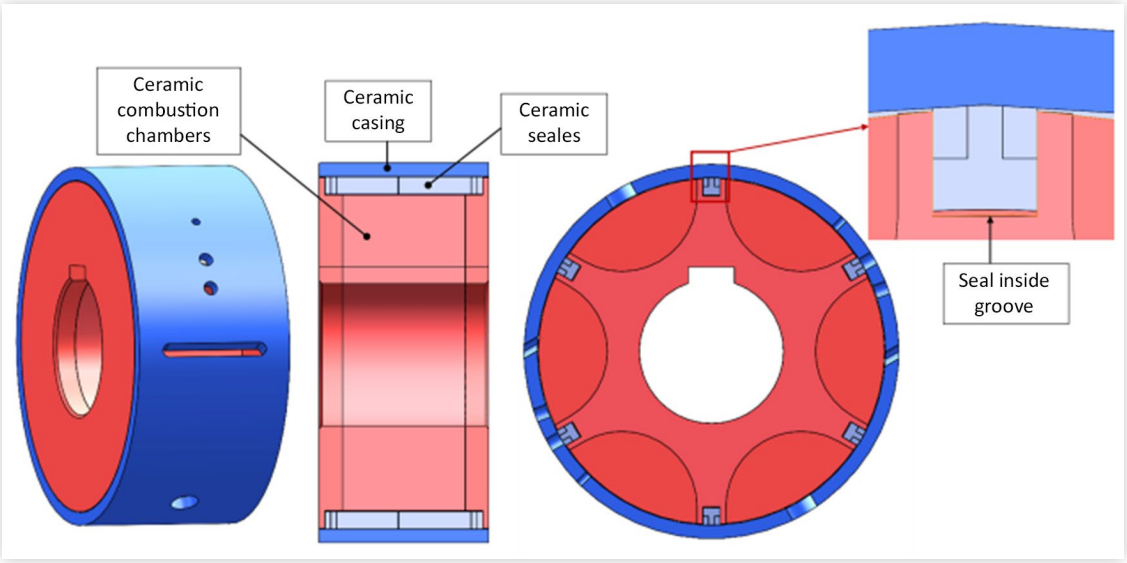

FIGURE 8 Combustion chambers with seals located in grooves (left), segment seals (right).

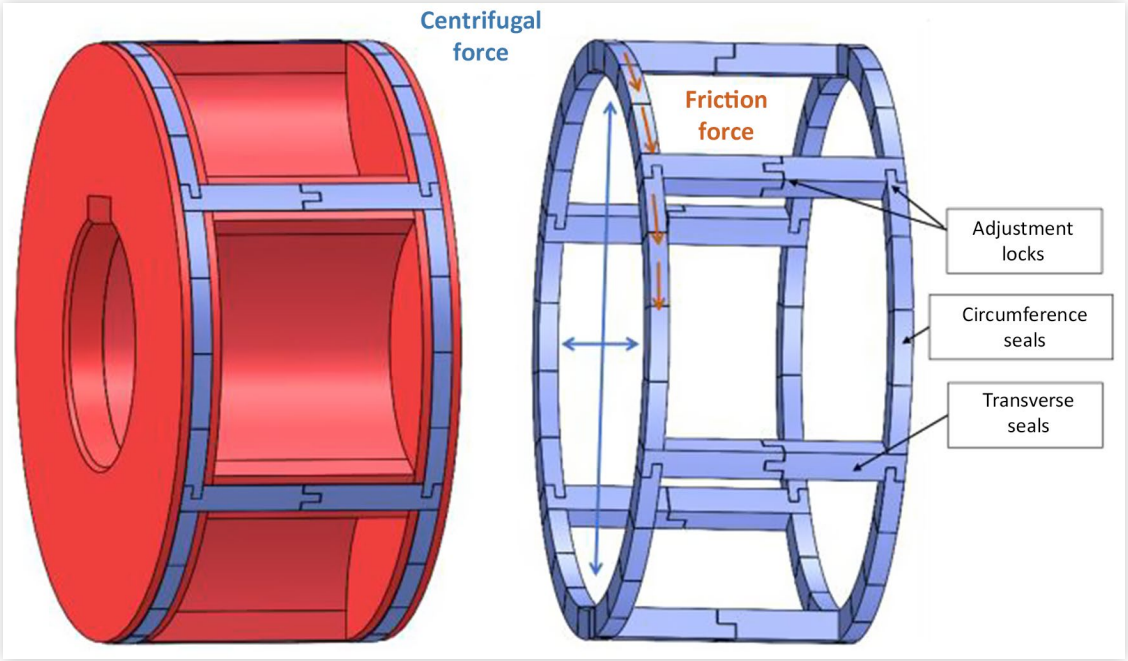

where F_f [N]—the force of friction, μ = 0.2 [–]—friction coefficient for a dry run, μ = 0.05 [–]—friction coefficient for a lubricated run [22, 23].

Friction work generated by the sealing system during dry operation was 3085.3 W, as calculated using Equation 3.

$$N_f = M_f \cdot \omega \tag{3}$$

where N_f [W]—work of friction, $M_f = F_f * R$ [Nm]—torque of friction, ω = 136.14 rad/s—rotational velocity of chambers.

The loss caused by friction is only 0.69% [24] of effective engine power (4).

$$L_f = \frac{N_f}{N_e} \cdot 100\% \tag{4}$$

where L_f [%]—percentage loss of friction, N_e = 444,600 W—effective engine power.

FIGURE 9 Sealing segments in offset position—Variant 1.

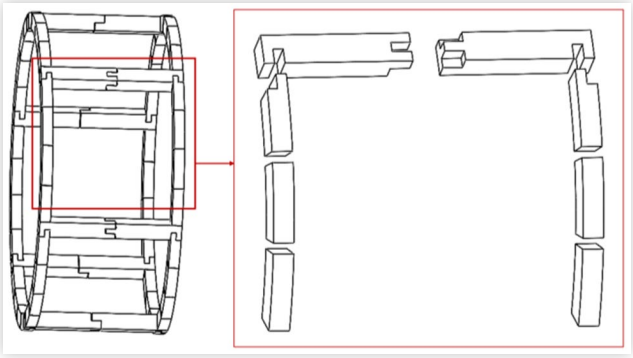

2.4. Segmentation of Seals

The seals are designed to have the same external diameter as the internal diameter of the casing. Under high-temperature conditions, both diameters will increase. Although the components are made with the same ceramic material (Si_3N_4), differences in geometry may lead to uneven thermal expansion, resulting in the formation of gaps. To minimize clearance between the seals and the casing, the seals should be divided into segments. For example, with a 0.2 mm difference between the seal and casing diameters, a maximum gap of 0.013 mm may appear in a segment with a 30-degree angular span, which is equivalent to two seal segments per chamber (see Figure 10). Reducing the segment span to 15 degrees (four segments per chamber) lowers the maximum gap to 0.0065 mm. In general, increasing the number of segments improves the conformity between mating surfaces and reduces the overall gap.

3. Results and Discussion

3.1. Technological Variants of Seals

Another interesting sealing solution is variant 2 presented in Figure 11. Instead of using locks in the transverse seal, half-cylinder curtains are introduced. These elements are positioned on both sides of the transverse seal. This solution, however, requires additional effort due to the need for machining more complex groove geometries.

FIGURE 10 Calculation of clearance between seals and casing.

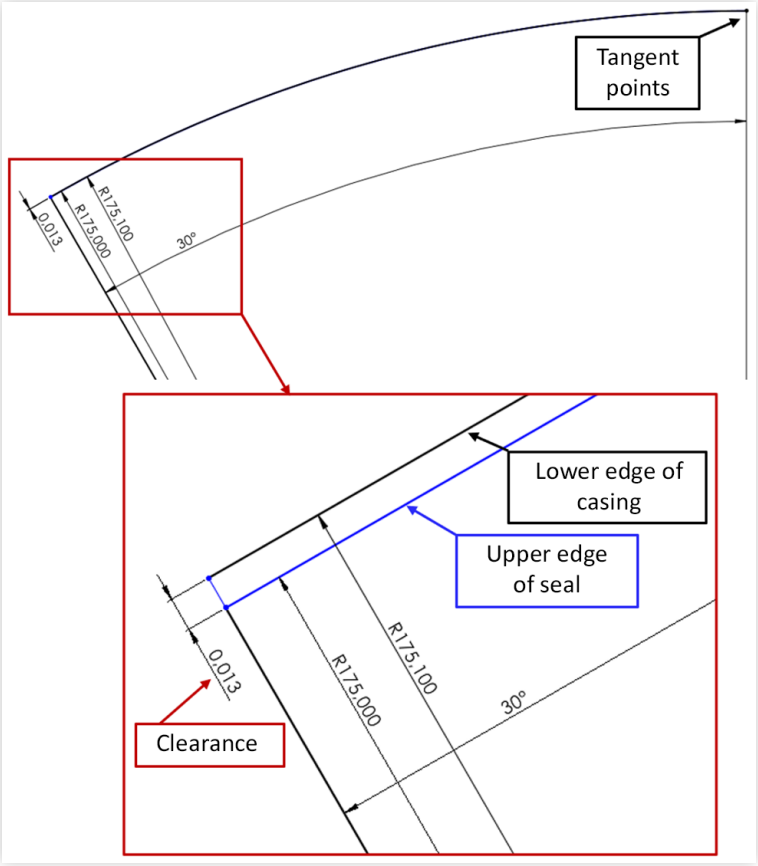

© Piotr Tarnawski

FIGURE 11 Variant 2 of the sealing system.

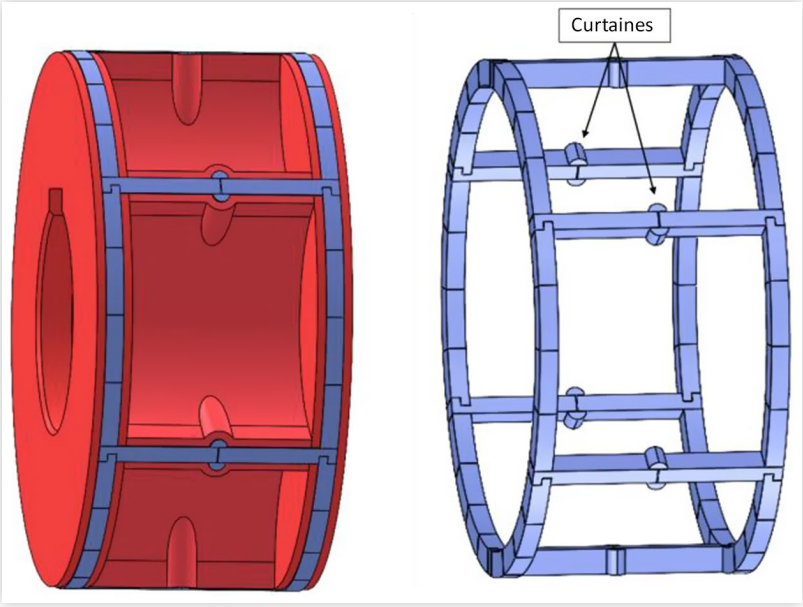

© Piotr Tarnawski

FIGURE 12 Construction of combustion chamber.

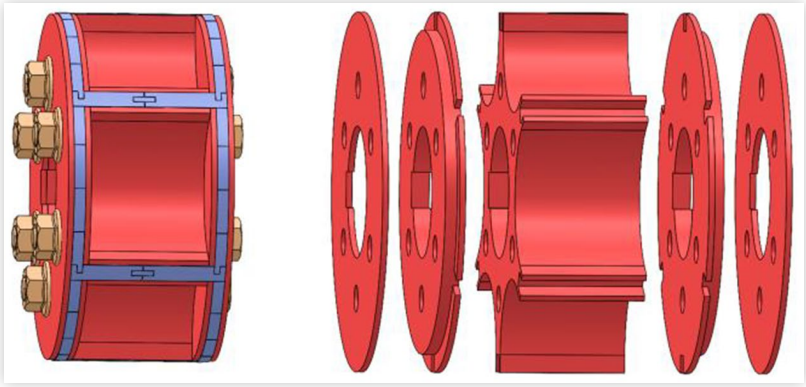

The effectiveness of sealing largely depends on the precision with which the sealing elements are manufactured. The width of the grooves should be approximately 0.002–0.003 mm greater than the width of the seals. Additionally, the surface roughness should be below Ra = 0.32 (Ra—arithmetic mean roughness). High manufacturing precision is essential to prevent high-pressure gas from leaking beneath the seals. Such leakage would lead to a pressure drop in the combustion chambers and increase the force by pressing the seals against the casing. Excessive pressing force would, in turn, raise friction, increase energy losses, and reduce the durability of the segmented sealing elements. The required level of machining accuracy for both seals and grooves necessitate the use of specialized techniques. Among them is the material abrasion method, which requires that the machined surfaces be pass-through. To accommodate this requirement, each combustion chamber should consist of five components, assembled using screws, as illustrated in Figure 12.

FIGURE 13 Construction of the lock of the transverse seal (modification of variant 1).

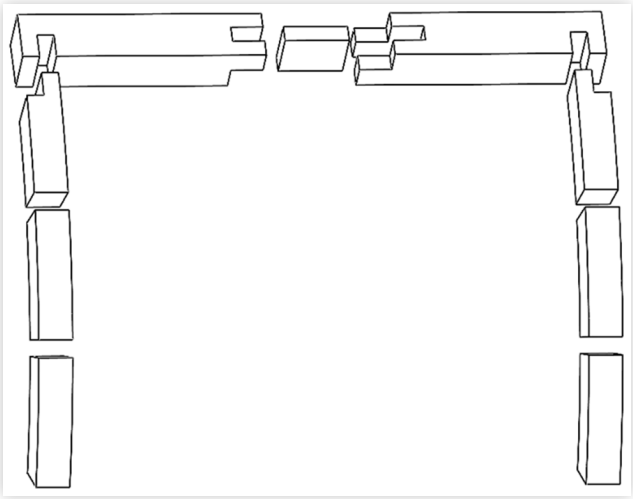

Similar machining requirements apply to the production of the seals themselves. The lock in the transverse seal should be composed of three elements, while the lock in the circumferential seal should consist of two elements. These specific requirements were consulted with the ceramic producer. The modification of variant 1 is shown in Figure 13.

3.2. Stand Model for Experimental Verification of Sealing Systems and Its Thermal Analysis

The proposed sealing system represents a critical component in the design of an engine with isochoric combustion chambers. Its effectiveness is essential for the successful implementation of the Humphrey thermodynamic cycle. Achieving a reliable seal in the isochoric combustion chambers is necessary to attain higher engine efficiency compared to conventional turboshaft engines currently available on the market. Experimental verification of self-adjusting segmented ceramic seals can be carried out using the model shown in Figure 14. This model incorporates a valve timing system with a single supply configuration, consisting of one inlet, one injector, and one exhaust port. The combustion chambers are intended to be driven by an electric motor, connected to the shaft via a clutch. The model does not include a turbine. Instead, a turbocharger will be used to extract power while simultaneously compressing the air required for combustion.

In order to assess the temperature distribution and determine the necessary cooling for the test stand model, a thermal analysis was conducted. After several design modifications, the model shown in Figure 15 was developed. Figure 15 presents the materials used, the thermal conductivities of the individual components and its surface emissivity.

The main design strategy was to minimize heat loss from the structure while simultaneously reducing the

FIGURE 14 Simplified geometry model of the engine for experimental verification of the sealing system.

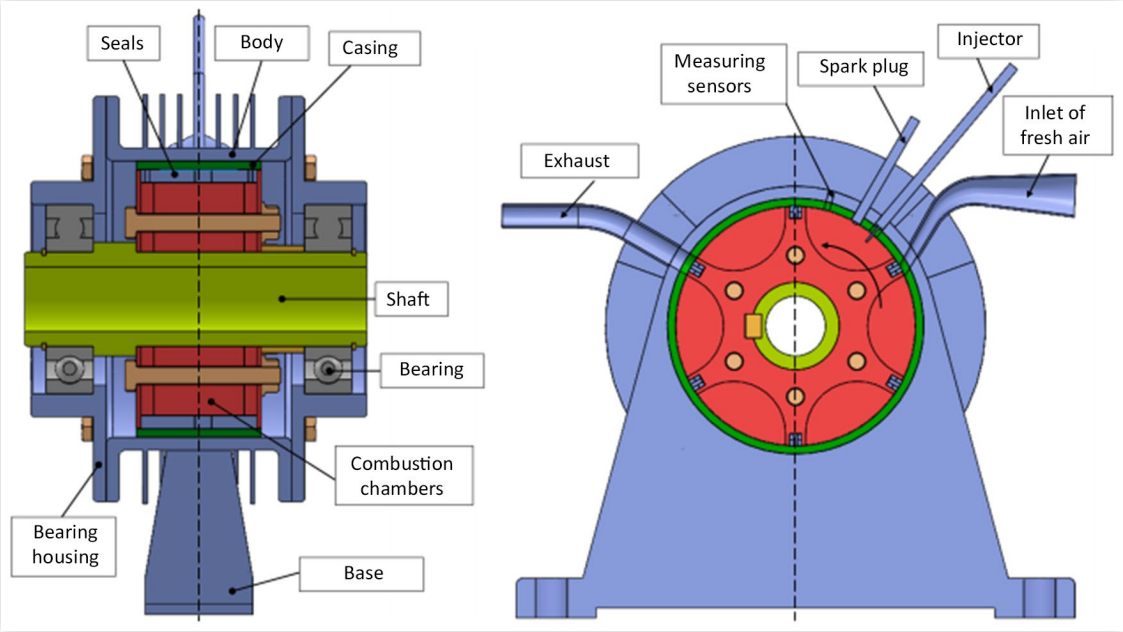

© Piotr Tarnawski

FIGURE 15 Selection of materials and boundary conditions.

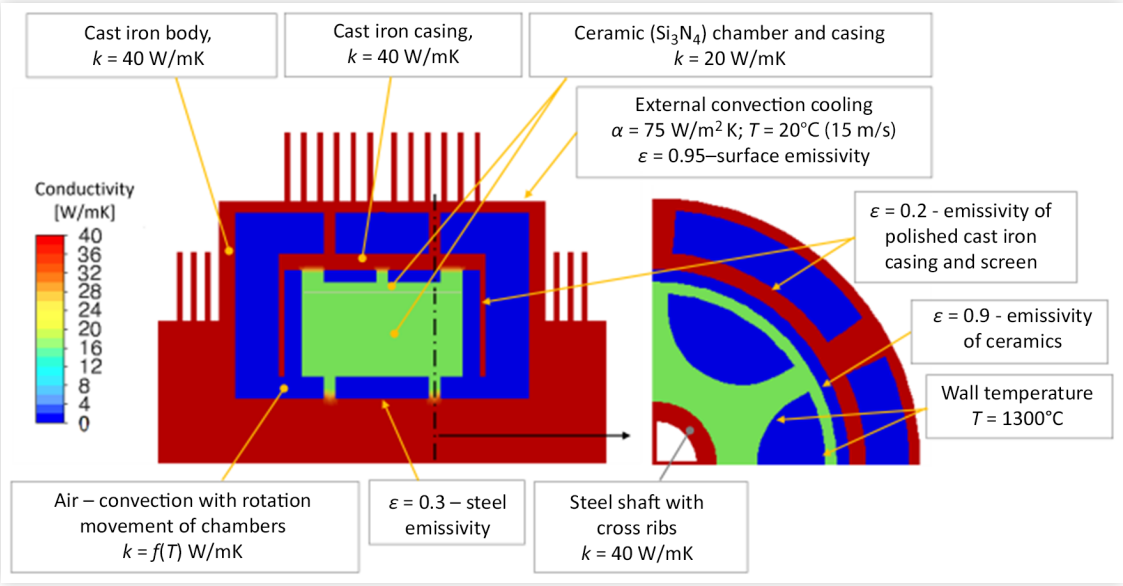

© Piotr Tarnawski

FIGURE 16 Numerical mesh of thermal model of valve timing system.

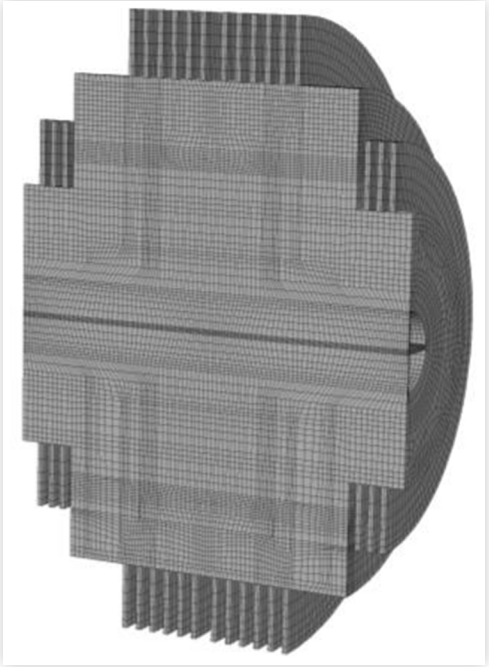

temperature of the external surfaces [25, 26]. To achieve this, the following steps were implemented:

- Minimizing of conduction heat transfer by reducing the contact area of the ceramic chambers with the shaft, the ceramic casing with the cast iron casing, and the cast iron casing with the cast iron body.
- Minimizing radiative heat transfer by the implementation of screens.
- Minimizing radiative heat transfer by polishing the surfaces (reduction of emissivity factor).
- Enhancing the heat transfer from external surfaces by the implementation of ribs.

The CFD thermal steady-state analysis was carried out using ANSYS Fluent software [27] with a mesh consisting of 204,783 hexahedral elements (see Figure 16).

The model was subjected to a boundary condition with a temperature of 1300°C, applied to the inner surfaces of the combustion chambers. Cooling of structure was achieved through forced airflow generated by a fan. The ambient temperature was set to 20°C, and the heat transfer coefficient was 75 W/m^2 K, corresponding to an air velocity of 15 m/s forced by the cooling fan (see Figure 10). As a result, the temperature of the cast iron components remained below 1100°C [28], meeting the material's thermal limits. The temperature of the external housing and the shaft ends remained below 250°C (see temperature distribution in Figure 17), which is acceptable for proper shaft bearing operation. The total heat flux removed by the cooling system was 5464 W, representing 4.4% of the fuel's chemical energy.

Tests of the operation of the sealing system should be performed in three stages:

- Without the load of pressure and temperature (dry run focused on the friction of seals),
- With only pressure load (the run with the gas flow from the compressor),
- With a load of pressure and temperature (the run included the injection of fuel and the combustion process).

The main parameters for verification are:

- Achieving a small resistance torque of the seals, generating no more than 2–3% of energy loss of the generated turbine work.
- Achieving seal durability of 600–800 hours of engine work without the need for replacement (it is the range for intermediate-level maintenance inspection for helicopters).
- Achieving a pressure increase in the chambers of at least two times the compression pressure [29, 30].

FIGURE 17 Temperature distribution in construction model for experimental verification of the sealing system.

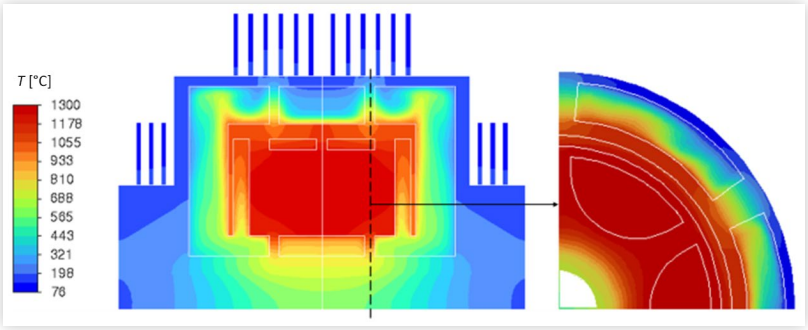

4. Conclusions

The self-adjusting segmented ceramic sealing system is an integral element of the presented engine concept, which operates according to the Humphreys cycle.

This engine concept is a very promising design. The numerically calculated efficiency exceeds that of conventional turboshaft engines currently available on the market.

The sealing system operates based on centrifugal force rather than the elasticity of the material. The sealing force is independent of pressure, temperature, or the associated material stiffness. As a result, the sealing force remains small and constant. The applied force produces low seal friction, amounting to just 0.69% of the engine's effective power. The relatively low load on each single-segment element (approximately 10 N) makes the sealing system potentially suitable for use throughout the required service interval without the need for replacement.

The sealing system features self-adjusting capabilities, maintaining consistent thickness regardless of thermal conditions and related deformations. Equipped with adjustment locks, the system can adapt its dimensions in both circumferential and transverse directions. The segmentation of the seals reduces potential clearances between differently deformed sealing and casing components.

In the event of gas leakage from the combustion chambers, the sealing system can temporarily enhance its self-adjusting mechanism. The solution involves temporarily interrupting the engine power supply (cutting off fuel injection), while simultaneously increasing the speed of the electric motor driving the combustion chambers. This action increases both the centrifugal and friction forces, which are responsible for adjusting the seals.

The production of the seals requires very high machining accuracy. The seal should be smaller than the grooves by approximately 0.002–0.003 mm. The surface roughness should be below Ra 0.32. For ceramic sealing elements, material abrasion methods need to be used. Therefore, the surfaces to be machined should be pass-through.

The sealing system concept has not been patented in order to allow interested companies and research centers to use this highly applicable solution for the sealing of isochoric combustion chambers in their own research and commercial applications. The article supports open innovation and facilitates collaboration within both research and industrial environments, as it can accelerate technological progress.

The experimental verification of a self-adjusting segmented ceramic sealing system is indispensable for the future of the presented engine concept. This verification can be performed using a simplified engine model (Figure 14). This design is optimal, as it allows for testing the tightness of the combustion chambers at the lowest possible cost.

Contact Information

Piotr Tarnawski
piotr.tarnawski@pw.edu.pl

References

1. Tarnawski, P., "Pulse Powered Turbine Engine Concept," Doctoral dissertation, Warsaw University of Technology, Warsaw, 2018.
2. Tarnawski, P. and Ostapski, W., "Pulse Powered Turbine Engine Concept Implementing Rotating Valve Timing System: Numerical CFD Analysis," *Journal of Aerospace Engineering* 32, no. 3 (2018): 1-13, 04019017.
3. Tarnawski, P., "The Hybrid Concept of Turboshaft Engine Working according to Humphrey Cycle Dedicated to Variety Power Demand – CFD Analysis," *Combustion Engines* 193, no. 2 (2023): 129-136, doi:https://doi.org/10.19206/CE-162763.
4. Tarnawski, P. and Ostapski, W., "Rotating Combustion Chambers as a Key Feature of Effective Timing of Turbine Engine Working according to Humphrey Cycle – CFD Analysis," *Bulletin of the Polish Academy of Sciences* 70, no. 5 (2022): 1-7, doi:10.24425/bpasts.2022.143100.
5. Tarnawski, P. and Ostapski, W., "The Hybrid Concept of Turboshaft Engine Enhanced by Steam Cycle Using Waste Heat Recovery—Combined Analytical and Numerical Calculation of Its Efficiency," *SAE Int. J. Engines* 17, no. 6 (2024): 795-806, doi:https://doi.org/10.4271/03-17-06-0045.
6. Miller, J.K., *Turbo: Real World High-Performance Turbocharger System* (North Branch, MN: CarTech, 2008).
7. Gas Turbine Engines, "Aviation Week and Space Technology," accessed November 11, 2022, http://www.geocities.jp/nomonomo2007/AircraftDatabase/AWdata/AviationWeekPages/GTEnginesAWJan2008.pdf.
8. Litalien, C., "Pratt and Whitney Canada Turboshaft Engines Product and Technology Evolution," in *European Rotorcraft Forum 33*, Kazan, Russia, 2007.
9. Brophy, C. and Roy, G., "Benefits and Challenges of Pressure-Gain Combustion Systems for Gas Turbines," *Mechanical Engineering* 131, no. 3 (2009): 54-55, doi:doi.org/10.1115/1.2009-MAR-8.
10. Kurec, K., Piechna, J., and Gumowski, K., "Investigations on Unsteady Flow within a Stationary Passage of a Pressure Wave Exchanger by Means of PIV Measurements and CFD Calculations," *Applied Thermal Engineering* 112, no. 5 (2017): 610-620, doi:doi.org/10.1016/j.applthermaleng.2016.10.142.
11. Akbari, P. and Nalim, M.R., "Review of Recent Developments in Wave Rotor Combustion Technology," *Journal of Propulsion and Power* 25, no. 4 (2009): 833-844, doi:doi.org/10.2514/1.34081.

12. Walraven, F., "Operational Behavior of a Pressure Wave Machine with Constant Volume Combustion," ABB Technical Report CHCRC 94-10, 1994. Tatarstan, Russia September 11–13, 2007.
13. Akbari, P., Tait, Ch., and Brady, G., "Enhancement of the Radial Wave Engine," in *AIAA Propulsion and Energy 2019 Forum*, Indianapolis, IN, August 2019.
14. Piechna, J., "A Review of Shock Wave Compression Rotary Engine Projects, Investigations and Prospects," *Energies* 15, no. 24 (2022): 9353, doi:https://doi.org/10.3390/en15249353.
15. Burger, B. and Bargende, M., "The Isochoric Engine," SAE Technical Paper 2020-01-0796 (2020), doi:https://doi.org/10.4271/2020-01-0796.
16. Shkolnik, A., Littera, D., Nickerson, M., Shkolnik, N. et al., "Development of a Small Rotary SI/CI Combustion Engine," SAE Technical Paper 2014-32-0104 (2014), doi:https://doi.org/10.4271/2014-32-0104.
17. San Andrés, L., "Gas Labyrinth Seals: On the Effect of Clearance and Operating Conditions on Wall Friction Factors – A CFD Investigation," *Tribology International* 131 (2019): 363-376, doi:https://doi.org/10.1016/j.triboint.2018.10.046.
18. Przybyła, B. and Zapałowicz, Z., "Review of Sealing Methods," Scientific Papers of the Rzeszów University of Technology, 2015.
19. Derlukiewicz, D., "Method of Modeling of Thermo-Elastic Phenomena in Layered Ceramic Coatings," Doctoral dissertation, Wroclaw University of Technology, Wroclaw, 2006.
20. "High Temperature Coatings," accessed September 23, 2017, http://www.virginia.edu/ms/research/wadley/high-temp.html.
21. TOPSEIKO, accessed September 20, 2024, https://top-seiko.com/pl/works/material-cat/ceramics/alumina/.
22. Feldshtein, E., Laber, A., Devojno, O., and Yatskievich, O., "The Tribological Studies of Plasma-Sprayed Ceramic Coatings," *Quarterly Tribologia* 230, no. 2 (2010): 23-34.
23. Szeptycka, B. and Skrzyniowski, A., "The Tribological Investigations of the Hybrid Composite Ni-SiC-Fluoropolymer Layer," *Kompozyty (Composites)* 3 (2003): 8.
24. Dowkontt, J., *Theory of Thermal Engines* (Warszawa: Wydawnictwo Kmunikacji i Łączności, 1973).
25. Hong, S., Rui, W., Mingmin, C., Jiao, W. et al., "Optimization Sealing and Cooling to Control Gas Intrusion in a Floating-Wall Combustion Chamber," *Bulletin of the Polish Academy of Sciences* 72, no. 2 (2024), doi:10.24425/bpasts.2024.148836.
26. Murray, A.V., Ireland, P.T., and Romero, E., "Development of a Steady-State Experimental Facility for the Analysis of Double-Wall Effusion Cooling Geometries," *J. Turbomach* 141, no. 4 (2019): 041008, doi:https://doi.org/10.1115/1.4041751.
27. Theory Guide, ANSYS® Academic Associate CFD, Release 16.2, Help System; ANSYS, Inc., Canonsburg, PA, 2016.
28. Rączka, J. and Sakwa, W., *Cast Iron, Engineer's Handbook* (Warszawa: Wydawnictwo Naukowo Techniczne, 1986).
29. Seang-Wock, L., Han-Seung, L., Young-Joon, P., and Yong-Seok, C., "Combustion and Emission Characteristics of HCNG in a Constant Volume Chamber," *International Journal of Hydrogen Energy* 37, no. 1 (2012).
30. Rajesh, K., Siddhant, J., Gaurav, V., and Avinash, K., "Laser Ignition and Flame Kernel Characterization of HCNG in a Constant Volume Combustion Chamber," *Fuel* 190 (2017): 318-327.